Inorganic Chemistry

Article

pubs.acs.org/IC

Efficiency of Polyoxometalate-Based Mesoporous Hybrids as Covalently Anchored Catalysts

Faiza Bentaleb,[†,‡] Ourania Makrygenni,[†,‡] Dalil Brouri,[§,∥] Cristina Coelho Diogo,[⊥] Ahmad Mehdi,[#] Anna Proust,[†,‡] Franck Launay,*[,§,∥] and Richard Villanneau*[,†,‡]

[†]Sorbonne Universités, UPMC-Paris 06, UMR 8232, Institut Parisien de Chimie Moléculaire, 4 Place Jussieu, F-75005 Paris, France

[‡]CNRS, UMR 8232, Institut Parisien de Chimie Moléculaire, 4 Place Jussieu, F-75005 Paris, France

[§]Sorbonne Universités, UPMC-Paris 06, UMR 7197, Laboratoire de Réactivité de Surface, site Le Raphael, Bat. A/B, 3 rue Galilée, 94200 Ivry-sur-Seine, France

[∥]CNRS, UMR 7197, Laboratoire de Réactivité de Surface, site Le Raphael, Bat. A/B, 3 rue Galilée, 94200 Ivry-sur-Seine, France

[⊥]Sorbonne Universités, UPMC-Paris 06, IMPC FR CNRS 2482, Collège de France, 11 place Marcelin Berthelot, 75231 Paris Cedex 05, France

[#]UMR CNRS 5253 Institut Charles Gerhardt, Chimie Moléculaire et Organisation du Solide, Université Montpellier, cc1701, Place E. Bataillon 34095 Montpellier, France

Supporting Information

ABSTRACT: Polyoxometalate (POM) hybrids have been covalently immobilized through the formation of amide bonds on several types of mesoporous silica. This work allows the comparison of three POM-based mesoporous systems, obtained with three different silica supports in which either the organic functions of the support (amine vs carboxylic acid) and/or the structure of the support itself (SBA-15 vs mesocellular foams (MCF)) were varied. The resulting POM-based mesoporous systems have been studied in particular by high resolution transmission electronic microscopy (HR-TEM) in order to characterize the nanostructuration of the POMs inside the pores/cells of the different materials. We thus have shown that the best distribution and loading in POMs have been reached with SBA-15 functionalized with aminopropyl groups. In this case, the formation of amide bonds in the materials has led to the nonaggregation of the POMs inside the channels of the SBA-15. The catalytic activity of the anchored systems has been evaluated through the epoxidation of cyclooctene and cyclohexene with H_2O_2 in acetonitrile. The reactivity of the different grafted POMs hybrids has been compared to that in solution (homogeneous conditions). Parallels can be drawn between the distribution of the POMs and the activity of the supported systems. Furthermore, recycling tests together with catalyst filtration experiments during the reaction allowed us to preclude the hypothesis of a significant leaching of the supported catalyst.

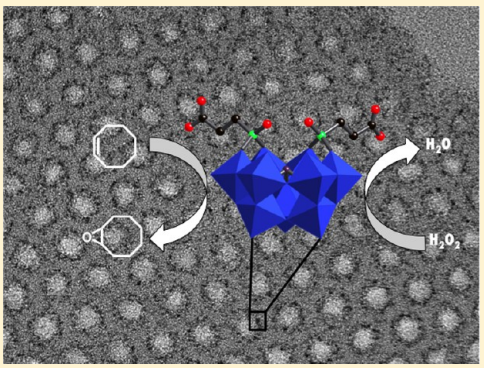

1. INTRODUCTION

Regarding their unique properties in terms of thermal stability, resistance toward oxidative conditions, and/or hydrolysis (provided that pH conditions are controlled), polyoxometalates (POMs) have been thoroughly considered as intrinsic oxidation catalysts either in homogeneous or heterogeneous conditions.[1−4] In the latter case, POMs are generally dispersed on oxide supports in order to circumvent their very low surface area in the solid state. In most examples, POMs are not strongly chemically bonded to the support. Studies generally involve either a simple physisorption or an electrostatic interaction with a positively charged support, acting like counterions.[3,5−10] This strategy has also been recently applied to surface-modified graphene.[11] POMs may also be immobilized successfully into materials through various other strategies[12] such as their encapsulation into metal−organic frameworks (MOFs),[13,14] their intercalation into layered double hydroxides,[15] or their one-pot embedding into a silica matrix via co-condensation sol−gel methods[16] (including the covalent grafting of vacant POMs into the walls of hybrid supports).[17,18]

We recently focused on the elaboration of new mesoporous materials functionalized with nucleophilic (vacant) POMs for applications in the field of anchored homogeneous catalysis.[19] In this preliminary work, we demonstrated, for the first time, that functionalization of both the vacant polyoxometalate species and the mesoporous silica support by complementary organic functions provides an efficient strategy for their covalent linkage. The principle was illustrated using an organophosphonate derivative of trivacant POMs bearing carboxylic acid functionalities on one hand and an NH_2-functionalized mesoporous SBA-15 support on the other hand

Received: May 29, 2015
Published: July 10, 2015

DOI: 10.1021/acs.inorgchem.5b01216
Inorg. Chem. 2015, 54, 7607−7616

(Figure 1). It is noteworthy that, following this report, such a strategy has been applied to the grafting of organosilyl

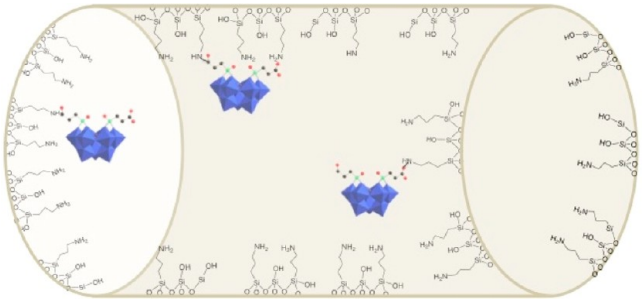

Figure 1. Covalent grafting of phosphonate derivatives of vacant POMs onto the walls of NH_2-functionalized SBA-15 silica. Counterions associated with the POMs are not represented for sake of clarity.

derivatives of Dawson-type POMs onto macroporous polymer matrices, via azide alkyne Huisgen cycloaddition.[20]

It is well-known that the efficiency of supported molecular catalysts is related not only to their accessibility but also to their dispersion and accessibility on the support. One of the keys for obtaining efficient materials are anchoring platforms with high specific surface and porosity, such as the SBA-15 silica used in our previous study.[19] However, an increasing number of inorganic supports are now available in the literature for catalysis purposes, with morphology and/or composition and/or surface modification that can now be easily modulated.[21,22] The effects of the modification of the support on the dispersion of the catalyst are thus questions we obviously need to address. Controlled immobilization of organometallic complexes in mesoporous silica has been reported.[23]

In the present work, we propose an extended study of the grafting of hybrids POMs on various organically modified supports. Three mesoporous supports have been examined, in which either the organic functions displayed (aminopropyl vs carboxypropyl) or the type of material itself, SBA-15 vs MCF (siliceous MesoCellular Foam), was varied. We thus analyzed both effects on the dispersion of the POMs in the different materials, in particular by high resolution transmission electronic microscopy (HR-TEM). In addition, the dispersion has then been tentatively correlated with the catalytic efficiency of the supported POMs in the cyclooctene and cyclohexene epoxidation by H_2O_2, used here as convenient model reactions.[24]

2. EXPERIMENTAL SECTION

2.1. Materials and Reagents. Solvents and other reagents were obtained from commercial sources and used as received, except for triethylamine and acetonitrile, which were distilled. The complexes $(^{n}Bu_4N)_3NaH[As^{III}W_9O_{33}\{P(O)(CH_2CH_2CO_2H)\}_2]$,[19] $TBA_3NaH(POM\text{-}CO_2H)$, and $(^{n}Bu_4N)_4H[PW_9O_{34}\{As(O)(C_6H_4NH_2)\}_2]$,[25,26] $TBA_4H(POM\text{-}NH_2)$, were prepared as previously described.

Solids were characterized by attenuated total reflection infrared spectroscopy, using Tensor R27 FTIR equipped with a ZnSe crystal with resolution better than 1 cm^{-1}. Raman spectra were recorded on solid samples on a Kaiser Optica Systems HL5R spectrometer equipped with a near-IR laser diode working at 785 nm. The ^1H (300.13 MHz), ^{13}C (75.6 MHz), and $\{^1H\}$ ^{31}P NMR (121.5 MHz) solution spectra were recorded in 5 mm o.d. tubes on a Bruker Avance 300 spectrometer equipped with a QNP probehead. ^{13}C CP MAS NMR spectra were recorded at 125.77 MHz on a Bruker AVANCE III 500 spectrometer (11.7 T) with a 4 mm Bruker probe and at a spinning frequency of 10 kHz (recycle delay = 5 s, contact time = 10 ms). ^{31}P MAS NMR spectra were recorded at 283.31 MHz on a Bruker AVANCE III 700 spectrometer (16.4 T) equipped with 2.5 mm Bruker probe and at a spinning frequency of 30 kHz. Chemical shifts were referenced to tetramethylsilane (TMS) for ^{13}C and to 85% aqueous H_3PO_4 for ^{31}P. Thermogravimetric analyses (TGA) were performed under air with a TA-Instrument SDT Q600 between 20 and 900 °C (air flow: 100.0 mL min^{-1}, 10 °C min^{-1}). Elemental analyses were performed by the Institut des Sciences Analytiques du CNRS (Villeurbanne, France). N_2 sorption analyses of the pretreated materials (100 °C) were obtained at −196 °C using an ASAP-2020 Micromeritics apparatus. Small-angle XRD measurements were carried out on a Bruker D8 Advance XRD diffractometer. X-ray fluorescence analyses were conducted with an energy dispersive spectrometer (XEPOS with Turboquant powder software). HR-TEM analyses were realized on a microscope operating at 200 kV with a resolution of 0.18 nm (JEOL JEM 2011 UHR) equipped with an EDX system (PGT IMIX-PC). Samples were dispersed in resin and cut with an ultramicrotome. The lamelas of 50 nm thickness were then deposited on Cu grid covered with an amorphous carbon film.

2.2. Preparation of the Functionalized Supports. *2.2.1. SBA-15 Silica with 3-Aminopropyl Groups (SBA-NH_2).*[19] $SBA\text{-}NH_2$ was obtained in a two-step procedure, after functionalization of a preformed SBA-15 with 3-aminopropyltriethoxysilane, as follows.

SBA-15 silica (1.0 g) previously dried at 350 °C for 12 h was dispersed in 50 mL of anhydrous toluene using an ultrasound bath for 5 min and magnetic stirring. Then, 3-(aminopropyl)triethoxysilane (APTES) (1 mL, 4 mmol) was added, and after 1 h, the resulting mixture heated up to 110 °C. Reflux was maintained for 24 h, after which the suspension was filtered. The recovered solid was washed with toluene, acetonitrile, and ethanol (15 mL of each), and then air-dried. The resulting $H_2N(CH_2)_3SiO_{1.5}/8SiO_2$ solid was extracted with dichloromethane using a Soxhlet for 24 more hours.

2.2.2. SBA-15 Silica with Carboxypropyl Functions (SBA-CO_2H).[27] $SBA\text{-}CO_2H$ support was prepared following a one-pot procedure synthesis: Pluronic 123 (4.0 g) was dissolved in 150 mL of an aqueous solution of HCl (pH ∼ 1.5). The resulting clear solution was then added to a mixture of (4-butyronitrile)triethoxysilane (BNTES) (1.04 g, 4.5 mmol) and tetraethylorthosilicate (TEOS) (8.40 g, 40.4 mmol). The mixture was vigorously stirred for 3 h at room temperature until a transparent solution appeared. The solution was transferred to a hot bath at 60 °C, and NaF (76 mg, 1.8 mmol) was immediately added. In the present case, NaF was acting as catalyst for polycondensation process. A white precipitate was formed after a few minutes. After aging under regular stirring for 3 days at 60 °C, the resulting powder was filtered off, and the surfactant was selectively removed by Soxhlet extraction with ethanol for 24 h. After the material was suspended in 25 mL of a 50 wt % H_2SO_4 and stirred at 120 °C for 5 h. Subsequently, the solid was recovered by filtration, washed with water and acetone and dried at 120°C under vacuum (0.1 mm Hg), $HOOC(CH_2)_3SiO_{1.5}/9SiO_2$ was obtained as a white powder.

2.2.3. MesoCellular Foam Silica with Aminopropyl Functions (MCF-NH_2). $MCF\text{-}NH_2$ was obtained in a two-step procedure, after functionalization of a preformed MCF[28] with 3-aminopropyltriethoxysilane, as follows.

First, Pluronic 123 (8.0 g) was added to 240 mL of distilled water and 40 mL of concentrated chlorhydric acid (37%). The mixture was heated at 40 °C until complete dissolution of Pluronic 123. Trimethylbenzene (9.2 mL, 8 g) was introduced dropwise as a swelling agent. After 2 h, TEOS (18 mL, 80 mmol) was also added dropwise, and the resulting suspension was further heated at 40 °C for 24 h. NH_4F (98 mg) was introduced 15 min before hydrothermal treatment. The latter was performed at 100 °C in a FEP bottle for an additional 24 h. The suspension was filtered, and the obtained solid was washed with water, dried at 60 °C, and finally calcined (24 °C min^{-1}) at 550 °C for 6 h.

Second, 1.0 g of freshly dried MCF silica (350 °C, 12 h) was added to 50 mL of anhydrous toluene. The resulting suspension was stirred at room temperature, and APTES (1.0 mL, 4 mmol) was introduced. After 2 h, the reaction mixture was heated until toluene reflux (110 °C) and maintained at this temperature for 24 h. Then, the suspension

DOI: 10.1021/acs.inorgchem.5b01216
Inorg. Chem. 2015, 54, 7607−7616

Table 1. Textural Data of the Supports before and after POM Coupling

	S_{BET} ($m^2\ g^{-1}$)	pore vol ($cm^3\ g^{-1}$)	pore diameter or window for MCF (nm) desorption	pore diameter or cell for MCF (nm) adsorption
SBA-NH_2	398	0.7	6.2	8.0
SBA-CO_2H	536	1.0	7.0	9.2
MCF-NH_2	327	1.5	7.1	17.4
POM-CO_2H@SBA-NH_2	185	0.33	4.7	7.0
POM-NH_2@SBA-CO_2H	477	1.0	6.2	9.2
POM-CO_2H@MCF-NH_2	245	1.0	6.2	17.3

was filtered. The recovered solid was washed successively with 15 mL of toluene, 15 mL of acetone, and then 15 mL of ethanol, and air-dried for 24 h. Finally, the solid was extracted using a Soxhlet during 24 h with dichloromethane as the solvent.

2.3. Covalent Binding of $TBA_3NaH(POM\text{-}CO_2H)$ with SBA-NH_2[19] and MCF-NH_2. Samples of $(^nBu_4N)_3NaH\text{-}[As^{III}W_9O_{33}\{P(O)(CH_2CH_2CO_2H)\}_2]$ (0.66 g, 0.2 mmol) and SBA-NH_2 silica (0.60 g, 4 mmol g^{-1} (nominal) of $-NH_2$ groups) (or MCF-NH_2, 0.60 g, 4 mmol g^{-1} (nominal) of $-NH_2$ groups) were introduced in 100 mL Schlenk tubes and kept under vacuum overnight. The POM-CO_2H complex was dissolved under argon in 20 mL of freshly distilled acetonitrile. Triethylamine (164 μL, 0.12 g, 1.2 mmol) was then added and the resulting mixture cooled in an ice bath. After 30 min, isobutylchloroformiate (156 μL, 0.16 g, 1.2 mmol) was introduced, and the resulting solution was stirred for 30 min (solution 1). In parallel, SBA-NH_2 or MCF-NH_2 silica was dispersed in distilled acetonitrile (5 mL) in the other Schlenk tube under argon. Solution 1 was then transferred to the dispersion of the support via cannula. The resulting suspension was stirred overnight at room temperature under argon, and then filtered. The recovered solid, i.e., POM-CO_2H@SBA-NH_2 or POM-CO_2H@MCF-NH_2, was finally extracted using a Soxhlet over 2 days with acetonitrile as the solvent. Chem Anal.: POM-CO_2H@SBA-NH_2: W(%) 19.12; Si(%) 23.08. POM-CO_2H@MCF-NH_2: W(%) 14.55; Si(%) 26.20.

2.4. Covalent Binding of $TBA_4H(POM\text{-}NH_2)$ with SBA-CO_2H. Samples of $(^nBu_4N)_4H[PW_9O_{34}\{As(O)(C_6H_4NH_2)\}_2]$ (0.26 g, 0.078 mmol) and SBA-CO_2H (0.5 g, 1.5 mmol g^{-1} of $-CO_2H$ groups) were each introduced in a 100 mL Schlenk tube and kept under vacuum overnight. The SBA-CO_2H support was then placed under argon with 10 mL of freshly distilled acetonitrile, and then *N*-hydroxysuccinimide (NHS; 1.8 mmol; 0.207 g) and 1-(3-(dimethylamino)propyl)-*N*′-ethylcarbodiimide hydrochloride (EDC; 0.9 mmol; 0.172 g) were successively introduced. The resulting suspension was stirred for 3 h at room temperature. In parallel, the $TBA_4H(POM\text{-}NH_2)$ complex was placed under argon and dissolved in 10 mL of freshly distilled acetonitrile. This solution was then transferred to the dispersion of the support using a cannula. The resulting suspension was stirred overnight at room temperature under argon, and then filtered. The solid recovered, i.e., POM-NH_2@SBA-CO_2H, was extracted using a Soxhlet over 2 days with acetonitrile as the solvent. Chem Anal.: W (%) 5.83; Si (%) 31.05.

2.5. Preparation of the POM-CO_2H-Supported on SBA-NH_2 Sample by Incipient Wetness Impregnation. A sample of SBA-NH_2 (0.5 g) with a pore volume of 0.7 mL g^{-1} was put in contact with 0.19 g of $TBA_3NaH(POM\text{-}CO_2H)$ in 0.35 mL of CH_3CN. After complete absorption of the liquid phase by the SBA-NH_2 support, the sample was dried under vacuum. It is noteworthy that the amount of POMs introduced was equal to the amount of POMs found in the final POM-CO_2H@SBA-NH_2 material obtained after covalent grafting (W: 19.2%, corresponding to 28.9% of anions $[As^{III}W_9O_{33}\{P(O)(CH_2CH_2CO_2H)\}_2]^{5-}$ (POM-CO_2H)).

2.6. Catalytic Studies. In homogeneous conditions, experiments of cyclooctene (or cyclohexene) epoxidation were performed in a 50 mL round-bottom flask equipped with a condenser and magnetic stirrer at room temperature or at 50 °C. The catalysts, $TBA_3NaH(POM\text{-}CO_2H)$ or $TBA_4H(POM\text{-}NH_2)$ (80 mg, 24 μmol/1 equiv), 20 mL of acetonitrile, 0.78 mL of cyclooctene or 0.60 mL of cyclohexene (6 mmol/250 equiv), 0.9 mL of decane (as an internal standard), and 0.6 mL of H_2O_2 (30%/6 mmol/250 equiv) were introduced successively in the flask. The resulting solutions were analyzed by gas chromatography on a Delsi Nermag DN 200 GC apparatus equipped with a flame ionization detector and a Macherey-Nagel Optima-5 capillary column (length 30 m, internal diameter 0.32 mm, thickness 1 μm).

In heterogeneous conditions, experiments of cyclooctene/cyclohexene epoxidation were performed in three 5 mL flasks (for analysis at 3, 6, and 24 h) under stirring at room temperature. The solid catalysts POM-CO_2H@SBA-NH_2 (40 mg), POM-NH_2@SBA-CO_2H (114 g), or POM-CO_2H@MCF-NH_2 (55 mg), corresponding to 1.2×10^{-3} mmol/1 equiv of POM-NH_2 or POM-CO_2H, 1 mL of acetonitrile, 39 μL of cyclooctene (250 equiv) or 30 μL of cyclohexene (250 equiv), 45 μL of decane, and 30 μL of H_2O_2 (30%, 250 equiv) were introduced successively in each flask. The supernatant of the resulting suspensions was analyzed by gas chromatography as described above. Blank reactions have been also performed with the different supports SBA-NH_2, SBA-CO_2H and MCF-NH_2, before the POMs-grafting steps. No catalytic activity was found for these materials in the absence of the POMs. For the recycling experiment, the catalyst has been filtered on a glass frit (por 4), rinsed with a few milliliters of CH_3CN, dried at air, and reused without any further treatments.

3. RESULTS AND DISCUSSION

In this work, three different POM-grafted materials were prepared in order to compare the nanostructuration of the active phase at the surface of the pores. These materials were obtained through the covalent binding of POM hybrids with three different functionalized mesoporous silica supports. In the continuity of our previous works, the strategy we used consisted of the coupling of complementary functions, one at the oxide-support and the second one on the termination of the organic groups introduced in the POM framework. In this respect, two different effects were studied: (1) the grafting reaction of POM hybrids on a given type of support (in the present case SBA-15 displaying anchoring aminopropyl or carboxypropyl functions); (2) the type of mesoporosity of the silica hosts, SBA-15 versus MCF, both functionalized with the same organic (aminopropyl) functions.

3.1. Characterization of SBA-NH_2, SBA-CO_2H, and MCF-NH_2 Materials. *3.1.1. Thermogravimetric Analyses.* The thermogram of SBA-NH_2 (see Supporting Information Figure S1) performed under air from room temperature up to 900 °C shows two weight losses. The first one (3%), under 100 °C, can be attributed to the loss of water molecules weakly adsorbed on the silica surface. The second one (17%, 100−800 °C) can be assigned to the loss of aminopropyl functions. This analysis demonstrated that SBA-NH_2 is functionalized with 3 mmol of NH_2 g^{-1} (ca. 75% incorporation yield).

Similarly, the thermogravimetric analysis of MCF-NH_2 exhibits two weight losses, respectively, of 2% and 15%. The second weight loss (100−800 °C) can still be attributed to aminopropyl functions. The MCF-NH_2 support was found to

DOI: 10.1021/acs.inorgchem.5b01216
Inorg. Chem. 2015, 54, 7607−7616

be functionalized by 2.3 mmol of NH_2 g^{-1} (ca. 60% incorporation yield). In comparison, the TGA-DTA analysis of SBA-CO_2H shows that it was functionalized with 1.7 mmol of $-CO_2H$ g^{-1} (ca. 100% incorporation yield).

3.1.2. Structural Study of SBA-NH_2, SBA-CO_2H, and MCF-NH_2 Materials. The X-ray powder diffraction patterns at 2θ (0.5−3°) of the SBA-NH_2 and SBA-CO_2H materials (see Supporting Information, Figure S2a,b) exhibited three peaks, the first one being far more intense than the other two. These signals were, respectively, assigned to the (100), (110), and (200) reflections of the expected hexagonal *P6m* structure. It is noteworthy that the intensities of the peaks related to the (110) and (200) reflections are smaller for SBA-CO_2H.

Transmission electron microscopy (TEM) confirmed the structure of SBA-NH_2 and SBA-CO_2H. The micrographs obtained by HR-TEM on both supports (see Supporting Information Figure S3) displayed the same organized tubular networks. Their textural data (see Table 1) were also comparable, although a larger specific surface was determined in the case of SBA-CO_2H. The micrographs of MCF-NH_2 confirmed the cellular foam structure of this support and the existence of cells with smaller apertures (windows) (Figure 2).

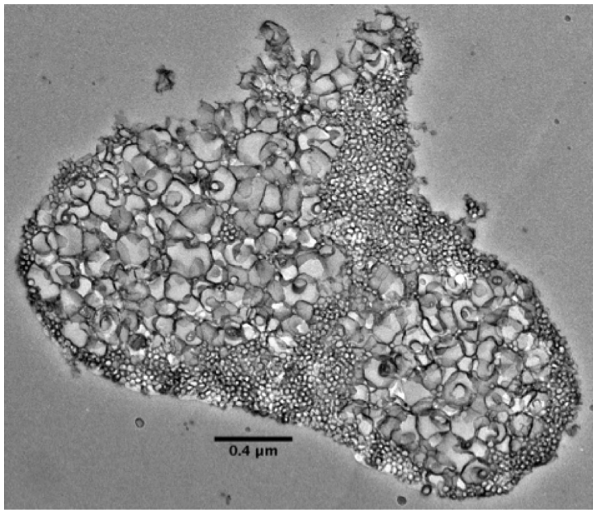

Figure 2. HR-TEM micrograph of MCF-NH_2 materials.

3.1.3. Nitrogen Physisorption. The nitrogen physisorption isotherms and the pore-size distribution of the two SBA supports are shown in Figure S4 (see Supporting Information). The adsorption/desorption isotherms are of type IV with a hysteresis loop. The pore sizes were calculated from the desorption branches of the isotherms using the Barret−Joyner−Hallenda (BJH) formula (Table 1). This method is used for the determination of the pore-size distribution of materials with pores larger than 4 nm, and it is appropriate for our silica supports (SBA-NH_2 and SBA-CO_2H). Values calculated from the adsorption branches were also determined in the case of MCF-NH_2 (Table 1).

3.2. Characterization Studies of the POM-Grafted Materials. Two different POMs, with organic functions complementary to those of the supports, were used: the previously reported $(^{n}Bu_4N)_3NaH[As^{III}W_9O_{33}\{P(O)(CH_2CH_2CO_2H)\}_2]$ complex, TBA_3NaH(POM-CO_2H), which contains two carboxylic acid functions, and the bis-anilino derivative TBA_4H(POM-NH_2), $(^{n}Bu_4N)_4H[PW_9O_{34}\{As(O)(C_6H_4NH_2)\}_2]$ (see Figure 3).[29]

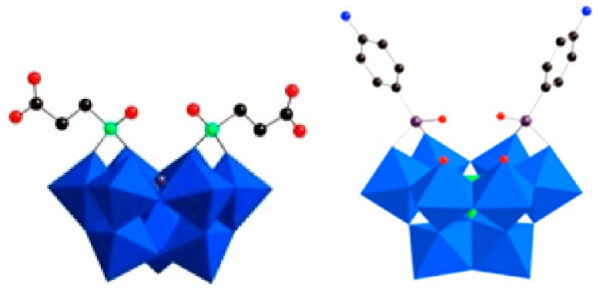

Figure 3. Structural representation of POM-CO_2H (left) and POM-NH_2 (right) anions. WO_6 and PO_4 polyhedra are shown in blue and green, respectively. The As, P, N, O, and C atoms are shown, respectively, in prune, green, blue, red, and black.

As previously reported,[19] the TBA_3NaH(POM-CO_2H) complex was easily grafted onto the NH_2-functionalized supports through the formation of amide bonds. For this purpose, isobutylchloroformiate (^{i}BuOC(O)Cl) was used as a coupling agent, in the presence of triethylamine. This procedure was repeated in the present work with SBA-NH_2 (POM-CO_2H@SBA-NH_2), and adapted also to MCF-NH_2 (POM-CO_2H@MCF-NH_2), which was not described until now. Both POM-functionalized amino supports were characterized by ^{13}C NMR (Supporting Information, Figure S5), ^{31}P CP-MAS NMR (Supporting Information, Figure S6), and Raman (Supporting Information, Figure S7) and IR spectroscopies, in order to confirm the integrity of the POMs after grafting and the formation of amide bonds (with ^{13}C CP-MAS NMR and IR). From this study, it was found that the spectra displayed similar patterns for both materials, in accordance with those previously reported.[19] Additionally, the powder X-ray diffraction patterns of POM-CO_2H@SBA-NH_2 (Supporting Information Figure S2c) displayed the diffraction peaks characteristic of the hexagonal structuration of the mesopores, indicating that the modified material kept the SBA-15 structure.

The second POM TBA_4H(POM-NH_2) contains two aniline functions.[26] The coupling procedure between these anilines and the carboxylic functions of the SBA-CO_2H was adapted from previous work done by some of us dealing with gold surfaces functionalized with carboxylic acid moieties (see section 2.4).[30] X-ray fluorescence (XRF) and chemical elemental analysis determined POM contents of the three materials at once. The obtained results are given in Table 2. It is worth noting that

Table 2. W/Si Molar Ratio and POM Content for POM-Grafted Materials

	W/Si molar ratio		
	XRF	elem anal.	POMs content (mmol g^{-1})
POM-CO_2H @SBA-NH_2	0.087	0.120	0.1
POM-NH_2 @SBA-CO_2H	0.020	0.028	0.035
POM-CO_2H @MCF NH_2	0.047	0.084	0.085

both techniques gave similar trends for the W/Si ratio, with the higher content in POMs being observed in the case of the $-NH_2$ functionalized supports. The POM contents (given in mmol per g of materials, based on the chemical elemental analysis results) are in the range 3.5×10^{-2} to 1×10^{-1} mmol g^{-1} of functionalized supports. This corresponds to the following POM loadings: (1) 9.2 wt % based on the anions $[PW_9O_{34}\{As(O)(C_6H_4NH_2)\}_2]^{5-}$ (POM-NH_2) for POM-

DOI: 10.1021/acs.inorgchem.5b01216
Inorg. Chem. 2015, 54, 7607−7616

NH_2@SBA-CO_2H, (2) 22.0 and 28.9 wt % based on the anions $[As^{III}W_9O_{33}\{P(O)(CH_2CH_2CO_2H)\}_2]^{5-}$ (POM-CO_2H), respectively, for POM-CO_2H@MCF-NH_2 and POM-CO_2H@SBA-NH_2.

POM-NH_2@SBA-CO_2H was also characterized by ^{31}P and ^{13}C CP-MAS NMR (see Supporting Information, Figure S8), and IR and Raman spectroscopies. Unfortunately, the significantly weaker content of POMs in POM-NH_2@SBA-CO_2H (W/Si molar ratio = 0.028 (0.02 by XRF), see Table 2) did not allow us to characterize the formation of amide bonds by all spectroscopies mentioned above.

Furthermore, textural data of this material were compared to those of POM-CO_2H@SBA-NH_2 and POM-CO_2H@MCF-NH_2. As expected, the greater the amount of POMs introduced (POM-CO_2H@SBA-NH_2), the greater the S_{BET} is decreased. We thus observed a significant diminution of the pore volume after grafting POM-CO_2H anions onto SBA-NH_2 materials, consistently with our previous results. Such low values of S_{BET} are generally observed for other POMs/SBA-15 systems obtained by classical POMs deposition, at high POMs loading.[31] On the other hand, the pore volume remained approximately constant in the case of POM-NH_2@SBA-CO_2H. It is worth noting that pore volumes and diameter variations may be hardly compared in the three materials since MCF structure is obviously different due to the presence of windows and cells.

3.3. High Resolution Transmission Electron Microscopy (HR TEM) of the POM-Grafted Supports. All three POM-grafted supports (POM-CO_2H@SBA-NH_2, POM-NH_2@SBA-CO_2H, and POM-CO_2H@MCF-NH_2) were characterized by high resolution TEM, after microtome cutting. The comparison between the supports before (see Figure 2 and Supporting Information Figure S3) and after POM grafting (Figures 4–6) was undoubtedly instructive. First of all, it can be observed at low magnification that the grafting of POMs did not alter the intrinsic structure of the supports, even in the presence of triethylamine.

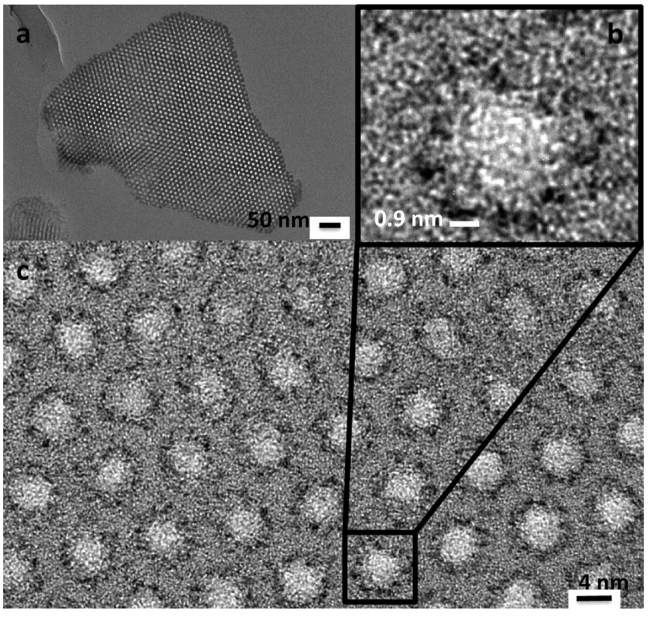

Figure 4. HR TEM micrographs (microtome cutting) of POM-CO_2H@SBA-NH_2 at different magnifications.

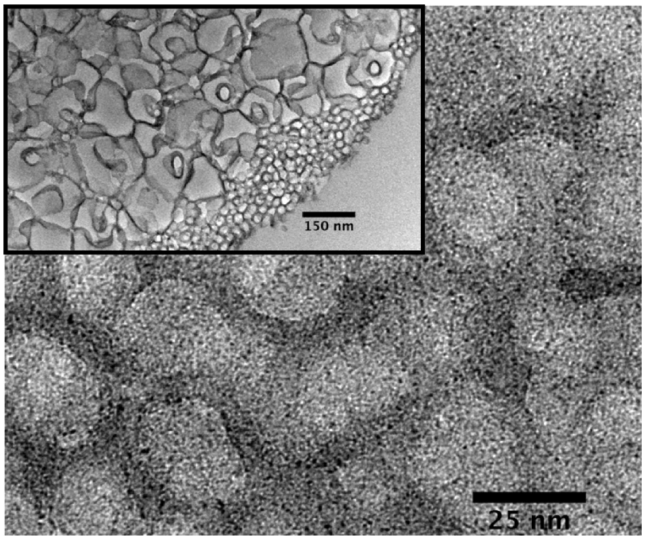

Figure 5. HR TEM micrographs (microtome cuttings) of POM-CO_2H@MCF-NH_2 at different magnifications.

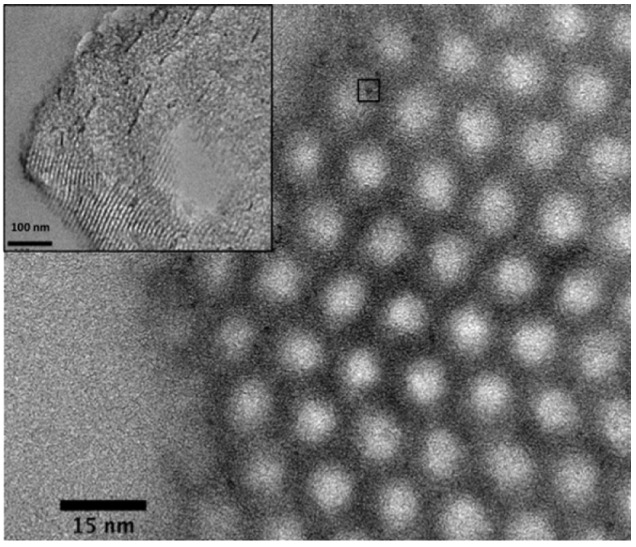

Figure 6. HR TEM micrographs (microtome cutting) of POM-NH_2@SBA-CO_2H at different magnifications.

By classical HR-TEM, the presence of POMs at the surface of the silica grains was not observed, even at high magnification. In contrast, microtome cuttings turned out to be a powerful tool, since it was possible to clearly identify the presence and, above all, the exact location of the POMs inside the pores or cells of the materials. In the case of POM-CO_2H@SBA-NH_2 (Figure 4), we clearly observed the regular distribution of POMs at the periphery of the channels. POMs appeared thus arranged in a monolayer in the pores, covering almost the whole inner surface. The efficiency of the microtome cutting, combined with the image contrast provided by heavy W atoms in the silica matrix, led us to consider that POMs did not form aggregates in these materials (average size of "dark" dots about 0.9 nm, Figure 4b). The covalent grafting of POMs onto the walls through the formation of amide functions led then to isolated anions and, thus, facilitated in a very efficient way the nanostructure of the catalysts on the support.

Examination of the elemental composition of a single grain of material by X-ray energy-dispersive spectroscopy (XEDS, see

DOI: 10.1021/acs.inorgchem.5b01216
Inorg. Chem. 2015, 54, 7607–7616

Supporting Information Figure S9 for more details) indicated that the ratio W/Si = 0.16 is on the same order of magnitude as that obtained by chemical analysis (W/Si = 0.12, Table 2). Moreover, XEDS also confirmed that the W atoms present in the solid were concentrated in the pores, with a measured W/Si ratio equal to 0.29 after deconvolution of the XEDS spectrum recorded on an area focused on one pore.

HR TEM micrographs of POM-CO_2H@MCF-NH_2 (Figure 5) also revealed the presence of POMs at the periphery of the cells. However, their distribution appeared less regular than in POM-CO_2H@SBA-NH_2 materials. This is obviously linked to the structure of the MCF silica, in which cells having walls with different intrinsic properties replaced cylindrical pores. Nevertheless, the size of the dots (attributed to the POMs) observed in all micrographs was mostly found to be around 1 nm. POMs still appeared as individual cluster anions, as observed in the case of POM-CO_2H@SBA-NH_2. As demonstrated in the previous materials, XEDS also confirmed that W atoms are mainly concentrated in the cells (Supporting Information, Figure S10).

HR-TEM micrographs of POM-NH_2@SBA-CO_2H (Figure 6) showed far fewer "dark" dots attributed to POMs, as expected due to the weakest POMs contents. Furthermore, while the distribution of POMs in the $-NH_2$ functionalized supports appeared regularly in every pore of the silica, in particular for POM-CO_2H@SBA-NH_2, we observed that only a few channels are covered with POMs (insert in Figure 6). In addition, the size of the POMs containing dots was evaluated, and it was found to be larger than that in the previous materials (about 1.8 nm for the dot inside the black square in the top of Figure 6, and larger ones were observed on several other micrographs). This suggests that POM-NH_2 anions were not found in the form of isolated species but preferably of aggregates of a few clusters. This makes us question the covalent grafting of POM-NH_2 at the surface of the SBA-CO_2H and, thus, the efficiency of the coupling procedure we used. XEDS was also performed on the materials, and we found that the W/Si ratio measured on a whole grain was identical (0.028) to the value found by chemical analysis. We also observed an increase of this value (up to 0.048) when the X-ray beam was concentrated on a single channel (Supporting Information, Figure S11). This increase led then to an unambiguous localization of the POMs in the SBA channels.

3.4. HR-TEM Study of Noncovalently Bound Anions POM-CO_2H in Mesoporous SBA-15. For this study, in order to point out the added value of the covalent grafting procedure for the POM organization, we prepared a different POM-CO_2H-supported SBA-NH_2 sample, obtained by incipient wetness impregnation of SBA-NH_2 with a solution (CH_3CN) of TBA_3NaH(POM-CO_2H). In this experiment, the amount of POMs introduced was equal to that found in the final POM-CO_2H@SBA-NH_2 materials obtained after covalent grafting (approximately 40% in mass), with the volume of solvent corresponding to the pore volume of the SBA-NH_2 used (0.7 $cm^3\ g^{-1}$). Several examples of HR-TEM micrographs obtained after microtome cutting are presented in Figure 7. First of all, we found by XEDS that the distribution of POMs was very irregular in the different grains of SBA-15. POMs were not present in all domains. Furthermore, in the case of POM-containing grains, POMs were generally not observed as isolated clusters (like in POM-CO_2H@SBA-NH_2 materials) but preferably as aggregates whose sizes were found in the 1.5−20 nm range. These micrographs also showed that some channels

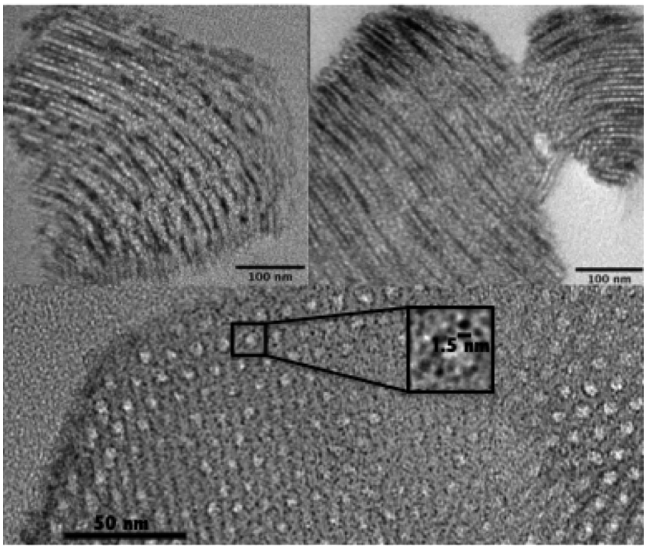

Figure 7. HR-TEM micrographs of SBA-NH_2 supports covered by TBA_3NaH(POM-CO_2H) after wet impregnation.

were not "filled" at all by POMs (see Figure 7, top left and right), on the contrary to what was observed previously in POM-NH_2@SBA-CO_2H samples. This seems to confirm that the nature of the interactions between POM-NH_2 anions and SBA-COOH was probably not covalent.

3.5. Comparative Study of the Catalytic Performance of Homogeneous vs Anchored Homogeneous Catalysts: The Case Studies of Cyclooctene/Cyclohexene Epoxidation with H_2O_2. *3.5.1. Epoxidation of Cyclooctene/Cyclohexene with H_2O_2 in Homogeneous Conditions.* Examples of the reactivity of heteropolytungstates that contain no additional transition-metal ions,[3,32] including organophosphonyle derivatives of POMs[33,34] in alkenes epoxidation processes can be found in the literature. Among all these studies, only one using organophosphonyle derivatives of trivacant POMs platforms was described so far, by the group of Bonchio.[33] Furthermore, the experimental conditions used in the present study may hardly be compared to those of Bonchio et al., who worked at very high temperature with microwave assistance.

Prior to the study of the catalytic performances of TBA_3NaH(POM-CO_2H) and TBA_4H(POM-NH_2) covalently supported onto mesoporous silica, we have checked the activity of the corresponding POMs under homogeneous conditions. The model reactions were, respectively, the epoxidation of cyclooctene and cyclohexene with aqueous H_2O_2 carried out at room temperature (excepted for some experiments specifically driven at 50 °C) in acetonitrile with the following catalyst/alkene/H_2O_2 ratio equal to 1:250:250. As expected, no reaction occurred in the absence of the catalysts, and we also checked that no H_2O_2 consumption was detected in the absence of cyclooctene/cyclohexene.

Cyclooctene Epoxidation. With both complexes, the conversion of cyclooctene into epoxycyclooctane in acetonitrile and at room temperature was observed with very high yields (respectively, 96% and 97%, see Table 3, entries 1 and 2) after 24 h. It is also noteworthy that, in all experiments described in this section, we did not detect products other than epoxycyclooctane, so it can be considered that the epoxycyclooctane selectivity was 100%. Differences between the two POMs were however shown for short time reaction

DOI: 10.1021/acs.inorgchem.5b01216
Inorg. Chem. 2015, 54, 7607−7616

Table 3. Epoxidation Conversion of Cyclooctene with Homogeneous and Anchored Catalysts[a]

entry	catalyst	T (°C)	3 h	6 h	24 h
1	$TBA_3NaH(POM\text{-}CO_2H)$	20	59.5	88.5	96
2	$TBA_4H(POM\text{-}NH_2)$	20	2.6	74	97
3	$TBA_3NaH[AsW_9O_{33}\{^tBuPO\}_2]$	20	0	2.4	7.5
4	$TBA_3NaH[AsW_9O_{33}\{^tBuPO\}_2]$	50	20.6	97	100
5	$TBA_4H[PW_9O_{34}\{PhPO\}_2]$	20	0.7	13.6	98
6	$POM\text{-}CO_2H@SBA\text{-}NH_2$	20	3.2	11.7	76
7	$POM\text{-}CO_2H@SBA\text{-}NH_2$ (recycling)	20	10.2	23	81
8	$POM\text{-}NH_2@SBA\text{-}CO_2H$	20	1	3.5	19
9	$POM\text{-}CO_2H@MCF\text{-}NH_2$	20	1	9	41
10	$POM\text{-}NH_2@SBA\text{-}CO_2H$	50	29	53	87

[a]Conditions: catalyst, 24 μmol (homogeneous conditions) or 1.2 μmol (heterogeneous conditions); acetonitrile, 20 mL (homogeneous conditions) or 1 mL (heterogeneous conditions). Ratio cyclooctene/catalyst = 250; cyclooctene/H_2O_2 (30%) = 1.

since a longer induction period seemed to be necessary for $TBA_4H(POM\text{-}NH_2)$ catalyst (conversion 2.6% after 3 h).

For the sake of comparison, we also tested the catalytic performances of two other compounds, $TBA_3NaH[AsW_9O_{33}\{tBuPO\}_2]$ (Table 3, entries 3 and 4) and $TBA_4H[PW_9O_{34}\{PhPO\}_2]$ (Table 3, entry 5) each related to $(^n\text{-}Bu_4N)_3NaH[AsW_9O_{33}\{P(O)(CH_2CH_2CO_2H)\}_2]$ ($POM\text{-}CO_2H$) and $(^n\text{-}Bu_4N)_4H[PW_9O_{34}\{As(O)(C_6H_4NH_2)\}_2]$ ($POM\text{-}NH_2$), respectively. The $TBA_4H[PW_9O_{34}\{PhPO\}_2]$ complex contains the same A,α-$\{PW_9O_{34}\}^{9-}$ anionic platform as $[PW_9O_{34}\{As(O)(p\text{-}C_6H_4NH_2)\}_2]^{5-}$ ($POM\text{-}NH_2$ anion), and two {As(O)Ph} groups instead of the $\{As(O)(p\text{-}C_6H_4NH_2)\}$ ones. The catalytic behavior of this compound was analogous to that of $TBA_4H(POM\text{-}NH_2)$, with a long induction time and a final conversion (after 24 h) close to 100% (Table 3, entry 5). We also compared the reactivity of $TBA_3NaH(POM\text{-}CO_2H)$ with that of $TBA_3NaH[AsW_9O_{33}\{^tBuPO\}_2]$ based on a B,α-$\{AsW_9O_{33}\}^{9-}$ subunit on which two $\{^tBuPO\}$ phosphonate groups have been grafted instead of the carboxypropyl functions in the $POM\text{-}CO_2H$ anion. In the present case, we found that, at room temperature, the behavior of both complexes was clearly different since the conversion after 1 day was found to be very low (7.5%) with $TBA_3NaH[AsW_9O_{33}\{^tBuPO\}_2]$ (Table 3, entry 3). It is noteworthy that an increase of the temperature up to 50 °C (Table 3, entry 4) led to a catalytic efficiency similar to that of $TBA_3NaH(POM\text{-}CO_2H)$. Regarding these results, we concluded that, at room temperature, the carboxylic functions of $POM\text{-}CO_2H$ anions could play a major role in the epoxidation process since the absence of these functions led to a dramatic decrease of the conversion of cyclooctene. These results could have been anticipated since the role of acids in general and of carboxylic acids in particular in epoxidation of alkenes (including cyclooctene) has been previously discussed in the literature, especially in POM chemistry.[35−37]

Cyclohexene Epoxidation. The epoxidation reaction of cyclohexene with aqueous H_2O_2 was also studied, with the conditions being adapted from those used for cyclooctene. We first checked the activity of $TBA_3NaH(POM\text{-}CO_2H)$ under homogeneous conditions in acetonitrile at room temperature. We thus found a good conversion of cyclohexene after 24 h (72.9%) and a final selectivity in the epoxide equal to 81.1%.[38] These results compare well with various other POM-based catalysts acting at room temperature (especially for the cyclohexene conversion rather than the selectivity).[32] For comparison, in acetonitrile at 50 °C, the Ishii−Venturello catalyst $(^n\text{-}Bu_4N)_3[PO_4\{WO(O_2)_2\}_4]$ produced cyclohexene epoxide with 98% selectivity at 84% conversion after 6 h.[39]

3.5.2. Epoxidation of Cyclooctene and Cyclohexene with H_2O_2 by the Covalently Anchored Catalyst $POM\text{-}CO_2H@SBA\text{-}NH_2$. The catalytic activity of the three different anchored catalysts ($POM\text{-}CO_2H@SBA\text{-}NH_2$, $POM\text{-}CO_2H@MCF\text{-}NH_2$, and $POM\text{-}NH_2@SBA\text{-}CO_2H$, see descriptions in sections 3.2 and 3.3) toward cyclooctene epoxidation was also studied (Table 3, entries 6, 8, and 9) in the conditions used for their homogeneous counterparts (section 3.5.1). The most efficient precursor was $POM\text{-}CO_2H@SBA\text{-}NH_2$ (Table 3, entry 6), in which the $POM\text{-}CO_2H$ anion was mostly grafted by only one carboxylic acid function, as established previously.[19] For this supported catalyst, the rate of cyclooctene conversion was still relatively high, even if it is lower compared to that obtained in homogeneous conditions (76% vs 96% after 1 day, see Figure 8). These differences were emphasized at an early stage (3.2% vs 59.5% after 3 h and 11.7% vs 88.5% after 6 h), reflecting an

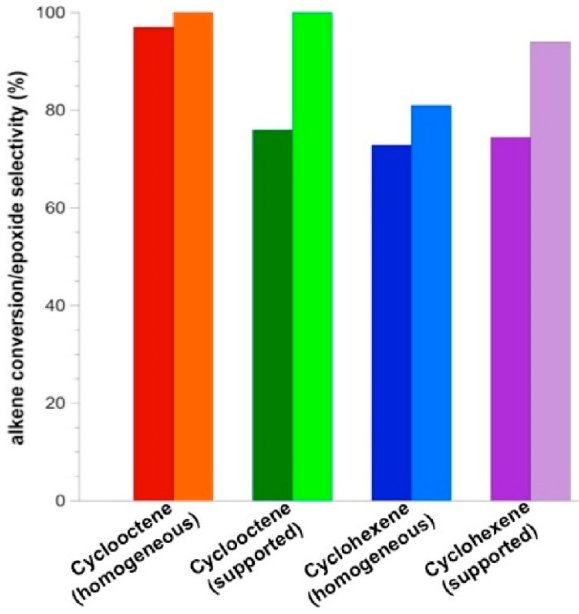

Figure 8. Column diagram for the alkene conversion (left bar) and epoxide selectivity (right bar) for (respectively, from left to right) cyclooctene with $TBA_3NaH(POM\text{-}CO_2H)$ in homogeneous conditions and $POM\text{-}CO_2H@SBA\text{-}NH_2$ in heterogeneous conditions and for cyclohexene with $TBA_3NaH(POM\text{-}CO_2H)$ in homogeneous conditions and $POM\text{-}CO_2H@SBA\text{-}NH_2$ in heterogeneous conditions.

DOI: 10.1021/acs.inorgchem.5b01216
Inorg. Chem. 2015, 54, 7607−7616

important delay probably due to different phenomena (lower diffusion rates of the substrate or different accessibility to the active sites in heterogeneous conditions). A recyclability test was also performed with the POM-CO_2H@SBA-NH_2 catalyst recovered after 24 h through filtration. Interestingly, we observed a similar (if not higher) cyclooctene oxide rate (81%) after 1 day, indicating an excellent stability of the catalyst.

The catalytic activity of the supported POM-CO_2H anion covalently bound to SBA-NH_2 (POM-CO_2H@SBA-NH_2) was also studied in the case of cyclohexene. Similarly to cyclooctene, significant delays were observed in the cyclohexene conversion at the early stage of the reaction. However, in the present case the final conversion was found to be on the same order (if not higher) as that observed in homogeneous conditions (72.9% for the homogeneous catalyst, i.e., TBA_3NaH(POM-CO_2H), vs 74.5% for the supported one). Interestingly, the final selectivity into epoxycyclohexane was much higher after immobilization (94.0% vs 81.1%).

Regarding the important delay observed at the beginning of the reaction in both experiments using POM-CO_2H@SBA-NH_2 and despite the fact that the experimental conditions used here (acetonitrile during 1 day at room temperature) were much more gentle than the initial catalyst treatment before its use (Soxhlet for 2 days in refluxing acetonitrile), it was important to determine the true nature of the catalysis. In other words, did POM-CO_2H@SBA-NH_2 behave as a supported catalyst or a homogeneous one obtained through (partial) leaching processes? Indeed, it is now admitted that a simple conventional catalyst recycling experiment showing no significant loss of activity (Table 3, entry 7) is by no means a sufficient proof of heterogeneity in itself. According to the procedures defined by R. A. Sheldon and co-workers,[40] the strong immobilization of the catalyst was proven through another experiment where (i) the POM-CO_2H@SBA-NH_2 catalyst was removed (filtration after 5 h with 0.2 μm porosity filters) before completion of the reaction (at room temperature) and (ii) the activity of the resulting filtrate was checked after 24 h. We then observed a dramatic lowering of the catalytic activity (see Figure 9) compared to the reference experiment (without filtration, see also Table 3, entry 6). Indeed while cyclooctene conversion was approximately 13.9% at the time of the filtration (at 5 h), the final conversion (at 24 h) within these experimental conditions hardly reached 25% versus 76% with the nonfiltered heterogeneous catalyst (Figure 9). We assume that the slight increase in the conversion after filtration (between 5 and 24 h) was probably due to the existence of remaining silica grains whose size was lower than 200 nm (size of the filter) in the solution, as observed by HR-TEM, instead of potential active species leached into solution. Nevertheless, regarding the results of the recyclability test and of the present experiment, one can be confident that the POM-CO_2H@SBA-NH_2 material can be considered as a truly anchored catalyst.

3.5.3. Epoxidation of Cyclooctene with H_2O_2. Comparison between Homogeneous and Covalently Anchored Catalysts. Concerning the catalytic activity of the other anchored catalysts, the scenario was surprisingly different with POM-CO_2H@MCF-NH_2 (Table 3, entry 9). After 1 day, only partial conversion of cyclooctene (41%) was observed, as the results of POM-CO_2H anion grafting onto a MCF-NH_2 instead of SBA-NH_2 support. With this experiment, we thus highlighted an effect of the support on the reaction rate. With the structure of

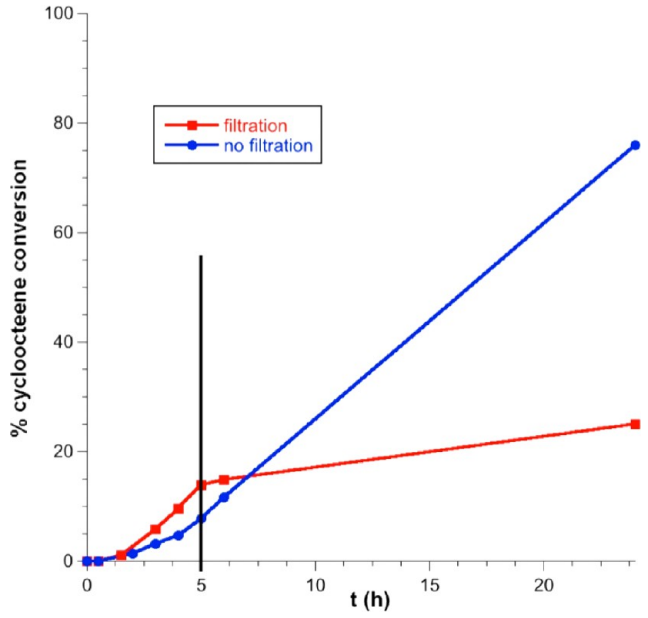

Figure 9. Catalytic activity of POM-CO_2H@SBA-NH_2 for the epoxidation of cyclooctene with aqueous H_2O_2 with (in red) or without (in blue) filtration. The black vertical line indicates the time for filtration.

the porosity being the main difference between SBA-NH_2 and MCF-NH_2 supports, it was tempting to hypothesize that variations of activity between POM-CO_2H@MCF-NH_2 and POM-CO_2H@SBA-NH_2 might be due to a poorer accessibility of the active sites in the particular case of MCF-NH_2. However, regarding the textural data, it is difficult to correlate *a priori* this decrease of the catalytic activity at the molecular level to the S_{BET} measured for both systems (lower for POM-CO_2H@SBA-NH_2 compared to for POM-CO_2H@MCF-NH_2, see Table 1). Another explanation could be related to the irregular organization of the active sites inside POM-CO_2H@MCF-NH_2 (see Figure 5) compared to those inside POM-CO_2H@SBA-NH_2 (see Figure 4) as shown by TEM micrographs. Existence of a tighter linkage (two carboxylic groups instead of one) between POM-CO_2H and MCF-NH_2 as the result of a surface geometry more adapted for multiple anchorage could also be invoked to explain the decrease of the reactivity of POM-CO_2H in POM-CO_2H@MCF-NH_2.

The existence of small aggregates as well as the irregular organization of POM-NH_2 in the third anchored catalyst, POM-NH_2@SBA-CO_2H, as shown in Figure 6, also had negative effects on cyclooctene conversion (Table 3, entry 8). Indeed, while in homogeneous conditions, we obtained a fair value after 1 day (97%), the conversion dramatically fell to 19% at ambient temperature in the case of POM-NH_2@SBA-CO_2H. Such a decrease is apparently due to a reduction of the exposed surface area of the active component of the catalyst and consequently a decrease of the contact between reactants and catalysts. POM-NH_2@SBA-CO_2H also culminated in the lowest POM loading of the three different anchored homogeneous catalysts so that significantly larger amounts of powder had to be used, leading to strong diffusion limitations. It is noteworthy that, for this specific solid material, a significant catalytic activity can be recovered at higher temperature (Table 3, entry 10).

The very encouraging results of the present study compare well with those obtained by Stein and co-workers.[17] Indeed, in

DOI: 10.1021/acs.inorgchem.5b01216
Inorg. Chem. 2015, 54, 7607−7616

their work, the incorporation of POM hybrids (derived from the γ-$[SiW_{10}O_{36}]^{8-}$ platform) by covalent links into porous silica materials had led to moderate yields (up to 28%) in the epoxidation of cyclooctene (at room temperature, after 24 h). Such comparison consequently validates the use of bisphosphonate derivatives of trivacant POMs for the preparation of anchored homogeneous catalysts. Indeed, we observed the persistence of fairly good catalytic activity after immobilization of the latter (probably due to the presence of "lacunary" oxygen atoms after grafting), provided that the best POM organization on the chosen support may be found.

4. CONCLUSION

In this work, we have prepared and characterized three POM-containing mesoporous silica supports and studied their catalytic activity in the epoxidation of cyclooctene and cyclohexene in the presence of hydrogen peroxide. These POM-anchored materials (POM-CO_2H@SBA-NH_2, POM-CO_2H@MCF-NH_2, and POM-NH_2@SBA-CO_2H) were obtained through amide coupling reactions between POMs hybrids and functionalized silica supports bearing each complementary pending group.

Two different POMs, with either carboxylic acid (TBA_3NaH-$[As^{III}W_9O_{33}\{P(O)(CH_2CH_2CO_2H)\}_2]$) or alkylamine functions ($TBA_4H[PW_9O_{34}\{As(O)(C_6H_4NH_2)\}_2]$), were used. Both POMs were shown to be efficient catalysts for cyclooctene epoxidation with aqueous H_2O_2 at room temperature in homogeneous conditions (acetonitrile). The bis-carboxylic acid derivative $TBA_3NaH[As^{III}W_9O_{33}\{P(O)$-$(CH_2CH_2CO_2H)\}_2]$ showed also interesting properties for the epoxidation of cyclohexene at room temperature, either in homogeneous conditions or after covalent immobilization on the SBA-NH_2 support, with an increased selectivity into epoxycylohexane in the latter case.

POM-anchored materials showed various catalytic performances in the epoxidation of cyclootene, with conversions in the range 19−97% after 24 h. These differences cannot be explained in terms of textural data since POM-CO_2H@SBA-NH_2, which presented the lowest S_{BET}, was also the best anchored catalyst. The POM organization throughout the materials appeared to be a determining parameter. The organization of the POMs at the pore (SBA-15) or cell (MCF) level of the materials that could be observed by HR-TEM (after microtome cutting) showed a decrease of the POM nanostructure from POM-CO_2H@SBA-NH_2 to POM-NH_2@SBA-CO_2H materials with some aggregates in the latter case. Trends emphasized for the catalytic activity of the anchored homogeneous catalysts were identical, i.e., the best activity for the material with the most ordered POMs.

Finally, recyclability experiments and a filtration test performed in the case of the POM-CO_2H@SBA-NH_2 (before completion of the cyclooctene epoxidation reaction) clearly indicated that this material can be considered as a truly anchored catalyst, thus precluding the hypothesis of significant leaching of the active species.

■ ASSOCIATED CONTENT

Supporting Information

Thermogravimetric analyses (TGA), weight losses, DTA curves and nitrogen adsorption/desorption isotherms of SBA-NH_2, SBA-COOH, and MCF-NH_2 materials. Powder X-ray diffraction patterns and TEM micrographs of SBA-NH_2, SBA-CO_2H, and POM-CO_2H@SBA-NH_2. ^{13}C CP-MAS NMR spectra of SBA-COOH, POM-NH_2@SBA-CO_2H, and POM-CO_2H@MCF-NH_2. ^{31}P CP-MAS NMR spectra of POM-CO_2H@SBA-NH_2 and POM-CO_2H@MCF-NH_2. Raman spectra of POM-CO_2H@SBA-NH_2 and POM-CO_2H@MCF-NH_2 compared to that of TBA_3NaH(POM-CO_2H). Details (HR-TEM) of the zones of POM-CO_2H@SBA-NH_2, POM-CO_2H@MCF-NH_2, and POM-NH_2@SBA-CO_2H functionalized silica grains studied by XEDS and tables indicating the W/Si contents. The Supporting Information is available free of charge on the ACS Publications website at DOI: 10.1021/acs.inorgchem.5b01216.

■ AUTHOR INFORMATION

Corresponding Authors

*E-mail: franck.launay@upmc.fr.

*E-mail: richard.villanneau@upmc.fr.

Author Contributions

The manuscript was written through contributions of all authors. All authors have given approval to the final version of the manuscript.

Notes

The authors declare no competing financial interest.

■ ACKNOWLEDGMENTS

The authors want to thank the Centre National de la Recherche Scientifique (CNRS) and the Université Pierre et Marie Curie (UPMC-Paris 06) for financial support, in particular for funding Dr Faiza Bentaleb as assistant lecturer, and for the Ph.D. fellowship to Miss Ourania Makrygenni. The authors want to thank Mrs. France Costa-Toro for help in ^{13}C CP MAS NMR spectroscopy. The French Région Ile de France—SESAME programs is acknowledged for financial support (700 MHz spectrometer).

■ REFERENCES

(1) Hill, C. L. Ed. Special Issue on Polyoxometalates in Catalysis. *J. Mol. Catal. A: Chem.* **2007**, *262*, 1−242.

(2) Kozhevnikov, I. Sustainable Heterogeneous Acid Catalysis by Heteropoly Acids. In *Handbook of Green Chemistry*; Anastas, P. T., Crabtree, R. H., Eds.; Wiley-VCH: Weinheim, 2009; Vol. 2, pp 153−174.

(3) (a) Mizuno, N.; Kamata, K. *Coord. Chem. Rev.* **2011**, *255*, 2358−2370. (b) Mizuno, N.; Kamata, K.; Yamaguchi, K. *Top. Catal.* **2010**, *53*, 876−893.

(4) Wang, S.-S.; Yang, G. Y. *Chem. Rev.* **2015**, *115*, 4893−4962.

(5) Kamada, M.; Kominami, H.; Kera, Y. *J. Colloid Interface Sci.* **1996**, *182*, 297−300.

(6) Vazylyev, M.; Slobodo-Rozner, D.; Haimov, A.; Maayan, G.; Neumann, R. *Top. Catal.* **2005**, *34*, 93−99.

(7) Rohlfing, D. F.; Rathousky, J.; Rohlfing, Y.; Bartels, O.; Wark, M. *Langmuir* **2005**, *21*, 11320−11329.

(8) Kato, C. N.; Tanabe, A.; Negishi, S.; Goto, K.; Nomiya, K. *Chem. Lett.* **2005**, *34*, 238−239.

(9) Kasai, J.; Nakagawa, Y.; Uchida, S.; Yamaguchi, K.; Mizuno, N. *Chem. - Eur. J.* **2006**, *12*, 4176−4184.

(10) Cheng, L.; Zhu, K.; Bi, L.-H.; Suchopar, A.; Reicke, M.; Mathys, G.; Jaensch, H.; Kortz, U.; Richards, R. M. *Inorg. Chem.* **2007**, *46*, 8457−8459.

(11) Quintana, M.; Montellano Lopez, A.; Rapino, S.; Maria Toma, F.; Iurlo, M.; Carraro, M.; Sartorel, A.; Maccato, C.; Ke, X.; Bittencourt, C.; Da Ros, T.; Van Tendeloo, G.; Marcaccio, M.; Paolucci, F.; Prato, M.; Bonchio, M. *ACS Nano* **2013**, *7*, 811−817.

(12) (a) Hill, C. L.; Kholdeeva, O. A. In *Liquid Phase Oxidation via Heterogeneous Catalysis: Organic Synthesis and Industrial Applications*; Clerici, M. G., Kholdeeva, O. A., Eds.; Wiley: Hoboken, NJ, 2013; pp

DOI: 10.1021/acs.inorgchem.5b01216
Inorg. Chem. 2015, 54, 7607−7616

263−319. (b) Kholdeeva, O. A.; Maksimchuk, N. V.; Maksimov, G. M. *Catal. Today* **2010**, *157*, 107−113.
(13) Salomon, W.; Yazigi, F.-J.; Roch-Marchal, C.; Mialane, P.; Horcajada, P.; Serre, C.; Haouas, M.; Taulelle, F.; Dolbecq, A. *Dalton Trans.* **2014**, *43*, 12698−12705.
(14) Maksimchuk, N. V.; Timofeeva, M. N.; Melgunov, M. S.; Shmakov, A. N.; Chesalov, Y. A.; Dybtsev, D. N.; Fedin, V. P.; Kholdeeva, O. A. *J. Catal.* **2008**, *257*, 315−323.
(15) Omwoma, S.; Chen, W.; Tsunashima, R.; Song, Y.-F. *Coord. Chem. Rev.* **2014**, *258*−*259*, 58−71.
(16) (a) Kholdeeva, O. A.; Vanina, M. P.; Timofeeva, M. N.; Maksimovskaya, R. I.; Trubitsina, T. A.; Melgunov, M. S.; Burgina, E. B.; Mrowiec-Bialon, J.; Jarzebski, A. B.; Hill, C. L. *J. Catal.* **2004**, *226*, 363−371. (b) Maksimchuk, N. V.; Melgunov, M. S.; Mrowiec-Białon, J.; Jarzebski, A. B.; Kholdeeva, O. A. *J. Catal.* **2005**, *235*, 175−183.
(17) Schroden, R. C.; Blanford, C. F.; Melde, B. J.; Johnson, B. J. S.; Stein, A. *Chem. Mater.* **2001**, *13*, 1074−1081.
(18) Zhang, R.; Yang, C. *J. Mater. Chem.* **2008**, *18*, 2691−2703.
(19) Villanneau, R.; Marzouk, A.; Wang, Y.; Ben Djamaa, A.; Laugel, G.; Proust, A.; Launay, F. *Inorg. Chem.* **2013**, *52*, 2958−2965.
(20) Xiao, Y.; Chen, D.; Ma, N.; Hou, Z.; Hu, M.; Wang, C.; Wang, W. *RSC Adv.* **2013**, *3*, 21544−21551.
(21) Hoffmann, F.; Cornelius, M.; Morell, J.; Fröba, M. *Angew. Chem., Int. Ed.* **2006**, *45*, 3216−3251.
(22) Pujari, S. P.; Scheres, L.; Marcelis, A. T. M.; Zuilhof, H. *Angew. Chem., Int. Ed.* **2014**, *53*, 6322−6356.
(23) Corriu, R. J. P.; Mehdi, A.; Reyé, C.; Thieuleux, C. *Chem. Commun.* **2003**, 1564−1565.
(24) Mouret, A.; Leclercq, L.; Mühlbauer, A.; Nardello-Rataj, V. *Green Chem.* **2014**, *16*, 269−278.
(25) Villanneau, R.; Racimor, D.; Messner-Henning, E.; Rousselière, H.; Picart, S.; Thouvenot, R.; Proust, A. *Inorg. Chem.* **2011**, *50*, 1164−1166.
(26) Villanneau, R.; Ben Djamâa, A.; Chamoreau, L.-M.; Gontard, G.; Proust, A. *Eur. J. Inorg. Chem.* **2013**, *2013*, 1815−1820.
(27) Folch, B.; Larionova, J.; Guari, Y.; Guérin, C.; Mehdi, A.; Reye, C. *J. Mater. Chem.* **2004**, *14*, 2703−2711.
(28) Schmidt-Winkel, P.; Lukens, W.; Zhao, D.; Yang, P.; Chmelka, B.; Stucky, G. *J. Am. Chem. Soc.* **1999**, *121*, 254−255.
(29) It is noteworthy that the POM platforms in both anions POM-CO_2H and POM-NH_2 are different: B,α-$[AsW_9O_{33}]^{9-}$ for POM-CO_2H, and A,α-$[PW_9O_{34}]^{9-}$ for POM-NH_2. The choice of these compounds has been done in order to maintain the presence of a ^{31}P nucleus in each POM hybrid for its characterization (^{31}P NMR), with the aniline function in POM-NH_2 being introduced through organoarsonate $\{As(O)(C_6H_4NH_2)\}$ groups, commercially available only in its arsonic form.
(30) Mercier, D.; Boujday, S.; Annabi, C.; Villanneau, R.; Pradier, C.-M.; Proust, A. *J. Phys. Chem. C* **2012**, *116*, 13217−13224.
(31) (a) Pinto, T.; Dufaud, V.; Lefebvre, F. *Appl. Catal., A* **2014**, *483*, 103−109. (b) Cuan, J.; Wang, B. *Microporous Mesoporous Mater.* **2014**, *183*, 9−16. (c) Kuang, W.; Rives, A.; Fournier, M.; Hubaut, R. *Appl. Catal., A* **2003**, *250*, 221−229. (d) Wang, J.; Zhu, H.-O. *Catal. Lett.* **2004**, *93*, 209−212. (e) Gao, R.; Zhu, Q.; Dai, W.-L.; Fan, K. *RSC Adv.* **2012**, *2*, 6087−6093.
(32) Mizuno, N.; Yamaguchi, K.; Kamata, K. *Coord. Chem. Rev.* **2005**, *249*, 1944−1956.
(33) Berardi, S.; Bonchio, M.; Carraro, M.; Conte, V.; Sartorel, A.; Scorrano, G. *J. Org. Chem.* **2007**, *72*, 8954−8957.
(34) Carraro, M.; Sandei, L.; Sartorel, A.; Scorrano, G.; Bonchio, M. *Org. Lett.* **2006**, *8*, 3671−3674.
(35) Sartorel, A.; Carraro, M.; Bagno, A.; Scorrano, A.; Bonchio, M.; Berardi, S. *J. Org. Chem.* **2007**, *72*, 8954−8957.
(36) Maheswari, P. U.; Tang, X.; Hage, R.; Gamez, P.; Reedijk, R. *J. Mol. Catal. A: Chem.* **2006**, *258*, 295−301.
(37) Kholdeeva, O. A.; Trubitsina, T. A.; Timofeeva, M. N.; Maksimov, G. M.; Maksimovskaya, R. I.; Rogov, V. A. *J. Mol. Catal. A: Chem.* **2005**, *232*, 173−175.
(38) As expected, the other products detected by GC correspond to *trans*-cyclohexane-1,2-diol (that came from the opening of the epoxycyclohexane with H_2O), a product typical of two-electron oxidation mechanisms, along with the classical allylic products (such as 2-cyclohexene-1-ol and 2-cyclohexene-1-one). It is noteworthy that the mass balance for this reaction (which was calculated after taking account of the initial reactive and all observed products in the chromatogram) was systematically found to be higher than 90% for each sampling, with a final mass balance after 1 day of 94%.
(39) (a) Venturello, C.; D'Aloisio, R.; Bart, J. C. J.; Ricci, M. J. *J. Mol. Catal.* **1985**, *32*, 107−110. (b) Matoba, Y.; Inoue, H.; Akagi, J.; Okabayashi, T.; Ishii, Y.; Ogawa, M. *Synth. Commun.* **1984**, *14*, 865−873. (c) Donoeva, B. G.; Trubitsina, T. A.; Maksimov, G. M.; Maksimovskaya, R. I.; Kholdeeva, O. A. *Eur. J. Inorg. Chem.* **2009**, *2009*, 5142−5147.
(40) Sheldon, R. A.; Wallau, M.; Arends, I. W. C. E.; Schuchardt, W. *Acc. Chem. Res.* **1998**, *31*, 485−493.

DOI: 10.1021/acs.inorgchem.5b01216
Inorg. Chem. 2015, 54, 7607−7616